Optimisation topologique d'interfaces microstructurées

Rémi Cornaggia,
Institut d'Alembert, Sorbonne Université, Paris, France

en collaboration avec **Marie Touboul** (Imperial College) et **Cédric Bellis** (LMA, Marseille)

Colloque MecaWave, 11 mai 2023

SORBONNE UNIVERSITÉ

∂'Alembert
Institut Jean le Rond d'Alembert

Microstructred interfaces and effective transmission conditions

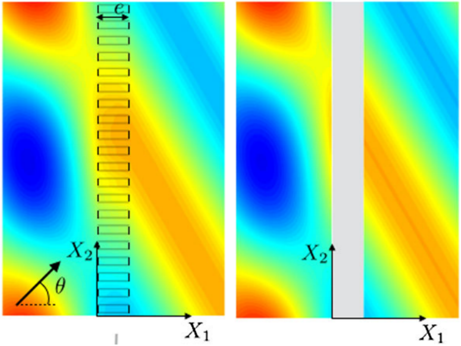

Frequency domain [Marigo et al., 2017]

$$k\ell = 0.5 \;\Rightarrow\; \ell/\lambda \approx 0.08$$

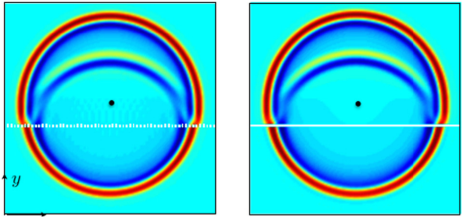

Time domain, rigid inclusions
[Lombard et al., 2017]

Multiple frequency signal $\Rightarrow\; \ell/\lambda \in [0.1, 0.6]$

Is it possible to *attenuate* or *enhance* the transmitted wave in some specific direction ?

An example from [Noguchi and Yamada, 2021]

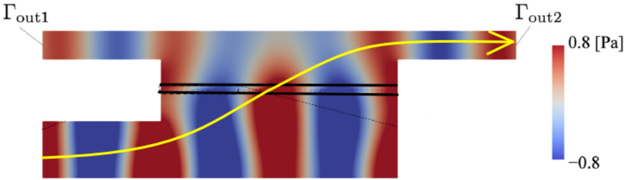

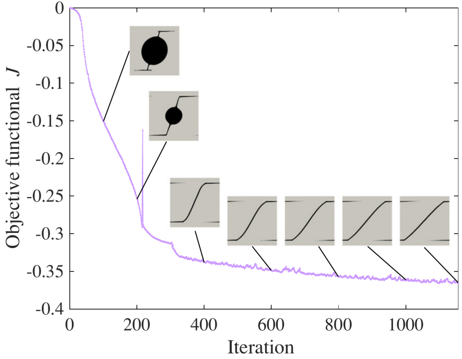

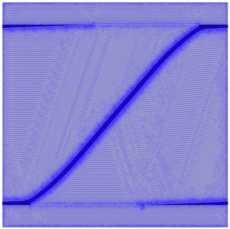

Noguchi, Y. & Yamada, T. *Topology optimization of acoustic metasurfaces by using a two-scale homogenization method* Applied Mathematical Modelling, 2021

Optimization based on an effective model

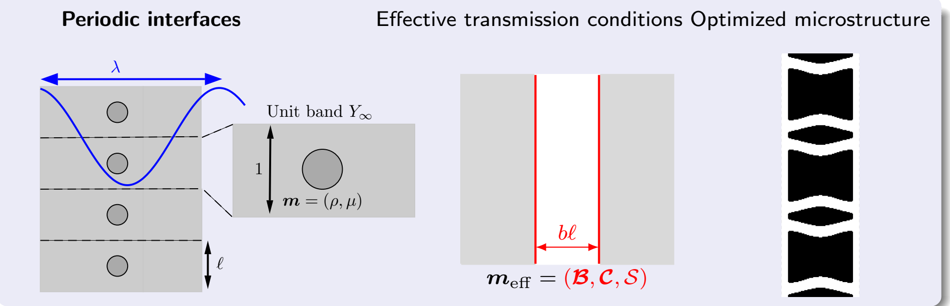

(1) Homogenization process toward effective transmission conditions:

- Double-scale expansions and matched asymptotics
- Band problems to capture the microstructural effects
- FFT-based solvers to address these problems

(2) Optimization strategy:

- Cost functionals based on effective transmission properties
- Topological sensitivity to drive updating steps
- Level-set representation, regularization and iterative algorithm
- Initialisation with optimal elliptic inclusions.

Outline

Effective transmission conditions [Marigo et al., 2017, Lombard et al., 2017]

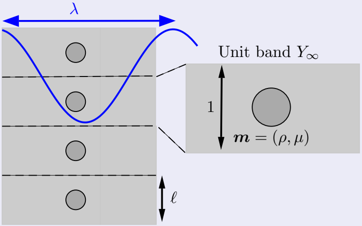

- Antiplane shear waves:

$$\rho\left(\frac{\boldsymbol{x}}{\ell}\right)\frac{\partial^2 u_\ell(\boldsymbol{x},t)}{\partial t^2} - \boldsymbol{\nabla}\cdot\left[\mu\left(\frac{\boldsymbol{x}}{\ell}\right)\boldsymbol{\nabla} u_\ell(\boldsymbol{x},t)\right] = 0$$

- (ρ, μ): density and shear modulus, 1-periodic along the interface
- **Long-wavelength** assumption: $\ell \ll \lambda$
- Double scale dependency and matched asymptotic expansions.

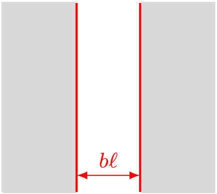

Effective model for **macroscopic fields** $(V, \boldsymbol{S})$:

$$\left|\begin{aligned}
&\rho_{\text{m}}\frac{\partial V}{\partial t} = \boldsymbol{\nabla}\cdot\boldsymbol{S} && |x_1| > \frac{b\ell}{2}\\
&\frac{\partial \boldsymbol{S}}{\partial t} = \mu_{\text{m}}\boldsymbol{\nabla} V && |x_1| > \frac{b\ell}{2}\\
&[\![V]\!]_{b\ell} = \ell\boldsymbol{\mathcal{B}}\cdot\langle\boldsymbol{\nabla} V\rangle_{b\ell}\\
&[\![S_1]\!]_{b\ell} = \ell\mathcal{S}\,\langle\boldsymbol{\nabla}\cdot\boldsymbol{S}\rangle_{b\ell} - \ell\boldsymbol{\mathcal{C}}\cdot\langle\boldsymbol{\nabla} S_2\rangle_{b\ell}
\end{aligned}\right.$$

Effective parameters computed from $\boldsymbol{\Phi}$, solution of a **band problem** on Y_∞.

Band problem

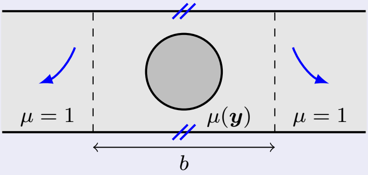

Original problem in **infinite band**:
(normalized "fast" coordinate $\boldsymbol{y} = \boldsymbol{x}/\ell$)

$$\begin{cases} \boldsymbol{\nabla} \cdot (\mu \, [\boldsymbol{I} + \boldsymbol{\nabla} \boldsymbol{\Phi}]) = \boldsymbol{0} \quad \text{in } Y_\infty \\ \boldsymbol{\Phi} \text{ is periodic in the } y_2 \text{ variable} \\ \lim_{y_1 \to \pm\infty} \boldsymbol{\nabla} \boldsymbol{\Phi} = \boldsymbol{0} \end{cases}$$

Computations in artificially bounded domain:

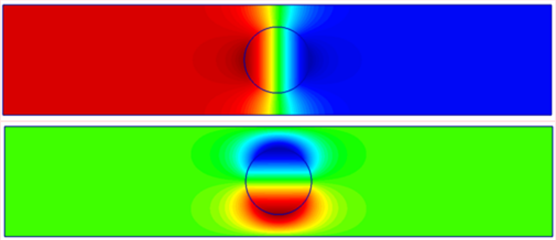

Effective coefficients [Marigo et al., 2017]

$$\mathcal{B} = \lim_{y_1 \to +\infty} \boldsymbol{\Phi} - \lim_{y_1 \to -\infty} \boldsymbol{\Phi} + \boldsymbol{f}(b)$$

$$\mathcal{C} = \int_{Y_\infty} \mu(\boldsymbol{y}) \partial_2 \boldsymbol{\Phi}(\boldsymbol{y}) \, \mathrm{d}\boldsymbol{y} + \boldsymbol{g}(b, \mu)$$

$$\mathcal{S} = h(b, \rho)$$

Reformulation as a cell problem [Cornaggia, Touboul & Bellis, *C. R. Mécanique*, 2022]

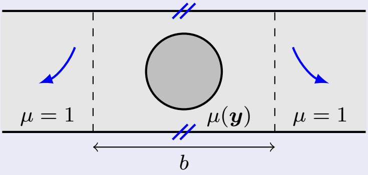

Original problem in **infinite band**:

$$\left| \begin{array}{l} \boldsymbol{\nabla} \cdot (\mu [\boldsymbol{I} + \boldsymbol{\nabla\Phi}]) = \boldsymbol{0} \quad \text{in } Y_\infty \\ \boldsymbol{\Phi} \text{ is periodic in the } y_2 \text{ variable} \\ \lim_{y_1 \to \pm\infty} \boldsymbol{\nabla\Phi} = \boldsymbol{0} \end{array} \right.$$

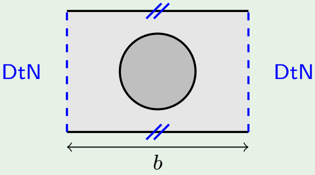

Equivalent cell problem:

$$\left| \begin{array}{l} \boldsymbol{\nabla} \cdot (\mu [\boldsymbol{I} + \boldsymbol{\nabla\Phi}]) = \boldsymbol{0} \quad \text{in } Y_b \\ \boldsymbol{\Phi} \text{ is periodic in the } y_2 \text{ variable} \\ \partial_n \boldsymbol{\Phi}(\pm b/2, \cdot) = \Lambda [\boldsymbol{\Phi}(\pm b/2, \cdot)] \end{array} \right.$$

Λ: **Dirichlet-to-Neumann (DtN)** operator.
$(\boldsymbol{\mathcal{B}}, \boldsymbol{\mathcal{C}})$ have expressions implying only integrals on Y_b

Numerical strategy: decomposition $\boldsymbol{\Phi} = \boldsymbol{\Phi}_{\text{per}} + \boldsymbol{\Phi}_{\text{bound}}$ (periodic + corrector)

- Λ and $\boldsymbol{\Phi}_{\text{bound}}$ have an **explicit expression** in Fourier basis.
- $\boldsymbol{\Phi}_{\text{per}}$ satisfies $\boldsymbol{\nabla} \cdot (\mu [\boldsymbol{I} + \boldsymbol{\nabla\Phi}_{\text{bound}} + \boldsymbol{\nabla\Phi}_{\text{per}}]) = 0$
  $\Longrightarrow$ iterative FFT-based solvers [Moulinec and Suquet, 1995]

Examples for an elliptic inclusion

$\mu_{\mathrm{inc}}/\mu_{\mathrm{mat}} = 6$, 129×129 pixels:

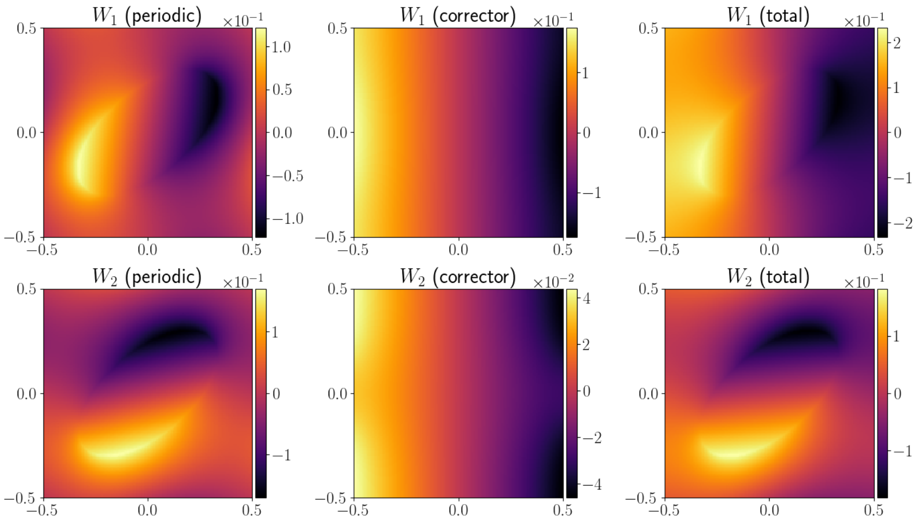

Outline

Cost functionals and optimization problem

Cost functionals: evaluate the medium performance through its **effective** properties:

$$\mathcal{J}(\boldsymbol{m}) = J(\boldsymbol{m}_{\text{eff}}) \qquad \text{here: } \begin{cases} \boldsymbol{m} = (\rho(\boldsymbol{y}), \mu(\boldsymbol{y})), \quad \boldsymbol{y} \in Y_b \\ \boldsymbol{m}_{\text{eff}} = (\boldsymbol{\mathcal{B}}, \boldsymbol{\mathcal{C}}, \mathcal{S}) \end{cases}$$

Examples : cost functionnals on **effective reflexion and transmission coefficients** for incident direction θ_{I} :

$$J(\boldsymbol{m}_{\text{eff}}) = F(\mathcal{R}(\boldsymbol{m}_{\text{eff}}, \theta_{\text{I}}), \mathcal{T}(\boldsymbol{m}_{\text{eff}}, \theta_{\text{I}}))$$

Optimization problem

Find $\boldsymbol{m}_{\text{opt}}$ that minimizes $\mathcal{J}(\boldsymbol{m})$.

With the dependencies $\boldsymbol{m} \to$ cell problems $\to \boldsymbol{m}_{\text{eff}} \to J(\boldsymbol{m}_{\text{eff}}) = \mathcal{J}(\boldsymbol{m})$

General strategy:

- Constraints and parametrization of $\boldsymbol{m}$, *e.g.* **piecewise uniform materials**
- **Iterative "material update" algorithms**

$$\boldsymbol{m}^{(n+1)} = \boldsymbol{m}^{(n)} + \Delta\boldsymbol{m}^{(n)} \quad \text{such that} \quad \mathcal{J}\left(\boldsymbol{m}^{(n+1)}\right) < \mathcal{J}\left(\boldsymbol{m}^{(n)}\right)$$

- Main tool: **sensitivity** of $\mathcal{J}$ to a material update $\Delta\boldsymbol{m}$ to choose a "good" $\Delta\boldsymbol{m}^{(n)}$.

Topological sensitivity of a cost functional

[Sokolowski and Zochowski, 1999, Garreau et al., 2001, Amstutz, 2011, Bonnet et al., 2018] ...

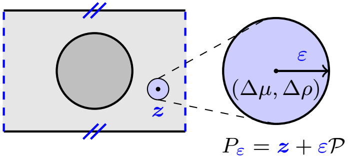

- **Localized phase change** in the cell: $\boldsymbol{m} \to \boldsymbol{m}_\varepsilon = \boldsymbol{m} + \chi_{P_\varepsilon}\Delta\boldsymbol{m}$

Expansion of $\mathcal{J}$: $\mathcal{J}(\boldsymbol{m}_\varepsilon) = \mathcal{J}(\boldsymbol{m}) + \varepsilon^2\,\mathcal{D}\mathcal{J} + o(\varepsilon^2)$ as $\varepsilon \to 0$

- $\mathcal{D}\mathcal{J}(\boldsymbol{m}; \boldsymbol{z}; \mathcal{P}, \Delta\mu, \Delta\rho)$: **topological sensitivity** (or gradient, or derivative) of $\mathcal{J}$.

If $\mathcal{D}\mathcal{J}(\boldsymbol{z}) < 0$, then $\mathcal{J}(\boldsymbol{m}_\varepsilon) < \mathcal{J}(\boldsymbol{m})$ and therefore $\boldsymbol{z}$ is a good choice for a phase change !

- **Chain rule** for $\mathcal{J}(\boldsymbol{m}) = J(\boldsymbol{m}_{\text{eff}})$:

$$\mathcal{D}\mathcal{J} = \frac{\partial J}{\partial \boldsymbol{m}_{\text{eff}}}\mathcal{D}\boldsymbol{m}_{\text{eff}}$$

$\Longrightarrow$ Need to compute $(\boldsymbol{\mathcal{D}\mathcal{B}}, \boldsymbol{\mathcal{D}\mathcal{C}}, \mathcal{D}\mathcal{S})$

Example : topological derivative of $\mathcal{S}$

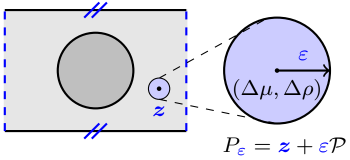

By definition :

$$\left|\begin{aligned} \mathcal{S} &= b + \frac{\rho_\mathrm{i} - \rho_\mathrm{m}}{\rho_\mathrm{m}}|\Omega_\mathrm{i}| \\ \mathcal{S}_\varepsilon &= b + \frac{\rho_\mathrm{i} - \rho_\mathrm{m}}{\rho_\mathrm{m}}|\Omega_\mathrm{i}| + \frac{\Delta\rho}{\rho_\mathrm{m}}|P_\varepsilon| \end{aligned}\right.$$

Exact expansion:

$$\mathcal{S}_\varepsilon = \mathcal{S} + \varepsilon^2 \underbrace{\frac{\Delta\rho}{\rho_\mathrm{m}}|\mathcal{P}|}_{\mathcal{DS}}$$

Here $\mathcal{DS}$ does not depend on $\boldsymbol{z}$ nor on the shape $\mathcal{P}$ (*not* the general case).

Topological derivatives and polarization tensor

The topological derivatives are (see [Touboul, PhD thesis, Chap. 4, 2021]) :

$$\mathcal{DS}(\boldsymbol{m}, \boldsymbol{z}, \mathcal{P}, \Delta \boldsymbol{m}) = \frac{\Delta\rho}{\rho_{\mathrm{m}}}|\mathcal{P}|,$$

$$\boldsymbol{\mathcal{DB}}(\boldsymbol{m}, \boldsymbol{z}, \mathcal{P}, \Delta \boldsymbol{m}) = -(\boldsymbol{\nabla}\Phi_1(\boldsymbol{z}) + \boldsymbol{e}_1) \cdot \boldsymbol{A}(\boldsymbol{z}) \cdot (\boldsymbol{\nabla}\boldsymbol{\Phi}(\boldsymbol{z}) + \boldsymbol{I}),$$

$$\boldsymbol{\mathcal{DC}}(\boldsymbol{m}, \boldsymbol{z}, \mathcal{P}, \Delta \boldsymbol{m}) = (\boldsymbol{\nabla}\Phi_2(\boldsymbol{z}) + \boldsymbol{e}_2) \cdot \boldsymbol{A}(\boldsymbol{z}) \cdot (\boldsymbol{\nabla}\boldsymbol{\Phi}(\boldsymbol{z}) + \boldsymbol{I}).$$

depend on

- the cell solution gradient at perturbation point $\boldsymbol{\nabla}\boldsymbol{\Phi}(\boldsymbol{z})$,
- the **polarization tensor** $\boldsymbol{A}(\boldsymbol{z}) = \boldsymbol{A}(\mathcal{P}, \mu(\boldsymbol{z}), \Delta\mu)$

Polarization tensor $\boldsymbol{A}$:

- used in [Cedio-Fengya et al., 1998, Ammari and Kang, 2007] in similar context,
- also called *localization* or *concentration* tensor, related to Eshelby and Hill tensors in elasticity/micromechanics [Eshelby, 1957, Parnell, 2016],
- symmetric,
- known analytically for **elliptic shapes** of semiaxes lengths (1,γ), and directions $(\boldsymbol{n}_1, \boldsymbol{n}_2)$:

$$\boldsymbol{A}^{\text{ellipse}}(\mu(\boldsymbol{z}), \Delta\mu) = \pi\gamma(\gamma+1)\frac{\Delta\mu}{\mu(\boldsymbol{z})}\left(\frac{\boldsymbol{n}_1 \otimes \boldsymbol{n}_1}{1+\gamma+\gamma\frac{\Delta\mu}{\mu(\boldsymbol{z})}} + \frac{\boldsymbol{n}_2 \otimes \boldsymbol{n}_2}{1+\gamma+\frac{\Delta\mu}{\mu(\boldsymbol{z})}}\right).$$

Numerical validation

- Leading-order approximation of homogenized coefficients e.g.

$$\boldsymbol{\mathcal{B}}_{\varepsilon} = \boldsymbol{\mathcal{B}} + \varepsilon^2 \boldsymbol{\mathcal{D}}\boldsymbol{\mathcal{B}}(\boldsymbol{z}) + o(\varepsilon^2)$$

- Computation of relative error e.g. :

$$\frac{\left|\mathcal{B}_{1,\varepsilon} - [\mathcal{B}_1 + \varepsilon^2 \mathcal{D}\mathcal{B}_1]\right|}{|\mathcal{B}_{1,\varepsilon}|}$$

(should be $o(\varepsilon^2)$, expected at least $O(\varepsilon^3)$)

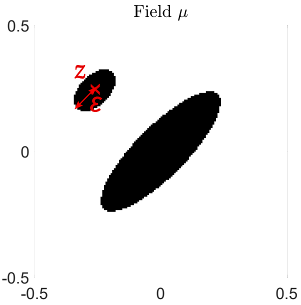

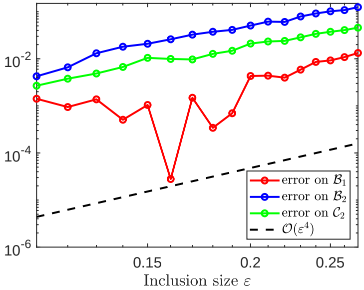

$\Longrightarrow$ Error in $O(\varepsilon^4)$ and $< 15\%$ (even for "big" perturbations $\varepsilon = 0.25$)
(term in ε^3 vanishes, should be true for *any centrally-symmetric* shape $\mathcal{P}$ [Bonnet, 2009])

Approximative effective coefficients for elliptic inclusions

Particular case: one inclusion P_ε in an **homogeneous** cell ($\mathbf{\Phi} = \mathbf{0}$)

$$\mathcal{S} = b + \varepsilon^2 \frac{\Delta\rho}{\rho_\mathrm{m}} |\mathcal{P}|, \quad \mathcal{B}_1 = b - \varepsilon^2 A_{11} + o(\varepsilon^2), \quad \mathcal{B}_2 = -\varepsilon^2 A_{12} + o(\varepsilon^2), \quad \mathcal{C}_2 = b + \varepsilon^2 A_{22} + o(\varepsilon^2).$$

- Analytical expressions when $\boldsymbol{A}$ is known
- Example : ellipse tilted at $40°$, semi-axes (ε, $0.2\,\varepsilon$):

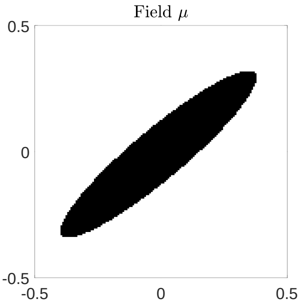

Case $\varepsilon = 0.5$

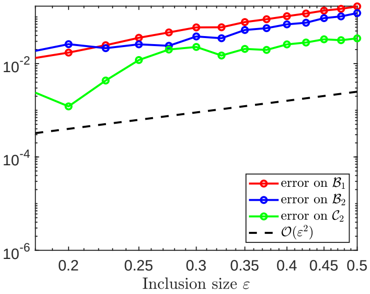

Relative error : $<$ 15% for $\varepsilon \leq 0.5$

Outline

Level-set representation and projection algorithm

[Amstutz and Andrä, 2006, Amstutz, 2011]

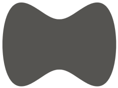

- Material distribution at iteration n represented by a **level-set function** ψ^n:

$$(\star)\begin{cases}\psi^n > 0 & \text{in } Y_1\\ \psi^n < 0 & \text{in } Y_2\end{cases} \quad \text{and} \quad \|\psi^n\|_{L^2(Y)} = 1$$

- Signed and normalized TD $\overline{\mathcal{D}}\mathcal{J}$ (here for $\mathcal{P}$ = disk):

$$\overline{\mathcal{D}}\mathcal{J} := \begin{cases}\mathcal{D}\mathcal{J}/\|\mathcal{D}\mathcal{J}\|_{L^2(Y)} & \text{in } Y_1\\ -\mathcal{D}\mathcal{J}/\|\mathcal{D}\mathcal{J}\|_{L^2(Y)} & \text{in } Y_2\end{cases} \quad \text{so that} \quad \|\overline{\mathcal{D}}\mathcal{J}\|_{L^2(Y)} = 1$$

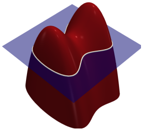

(Wikipedia)

Optimality condition: If $\overline{\mathcal{D}}\mathcal{J}$ satisfies the sign condition $(\star)$ then $\mathcal{D}\mathcal{J}(\boldsymbol{z}) > 0 \quad \forall \boldsymbol{z} \in Y$
then $\mathcal{J}$ reached a **local minimum**

Update of ψ by **projection** onto $\overline{\mathcal{D}}\mathcal{J}$:

$$\psi^{n+1} = a_n \psi^n + b_n \overline{\mathcal{D}}\mathcal{J}(\psi^n)$$

(a_n, b_n) are chosen so that $\|\psi^{n+1}\|_{L^2(Y)} = 1$ and $\mathcal{J}(\psi^{n+1}) < \mathcal{J}(\psi^n)$

A first test [Touboul, Ph.D. Thesis, 2021 (Chap. 4)]

- **Goal** : minimization of the effective reflexion coefficient $\mathcal{R}$ for an incident angle $\theta_{\mathrm{I}} = \pi/4$
  - Define $\mathcal{R}(\boldsymbol{m}_{\mathrm{eff}}, \theta_{\mathrm{I}})$ with $\boldsymbol{m}_{\mathrm{eff}} = (\boldsymbol{\mathcal{B}}, \boldsymbol{\mathcal{C}}, \mathcal{S})$
  - Compute the sensibilities $(\mathcal{D}\boldsymbol{\mathcal{B}}, \boldsymbol{\mathcal{DC}}, \boldsymbol{\mathcal{D}}\mathcal{S})$

- **Two-phase material:** (1) matrix and (2) inclusion.

- Volume constraint on inclusion phase Y_2 in the unit cell: $V_C = 0.6$

- Perimiter penalization following [Amstutz, 2013] to get smooth final configurations

$$\mathcal{J} = |\mathcal{R}|^2 + \lambda\left(\frac{|Y_2|}{V_C} - 1\right)^2 + \alpha_{\mathrm{per}}\mathrm{Per}(Y_2) \quad (\lambda\text{: iteratively chosen weight})$$

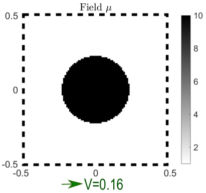

Initial unit cell

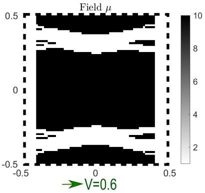

Final unit cell

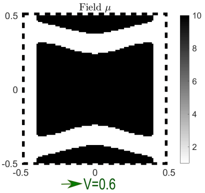

with perimeter penalization


Microstructure

Attenuated scattered field

- **Numerical experiments :** for a pulse emitted at a source point, measure the energy of the scattered field by the interface:

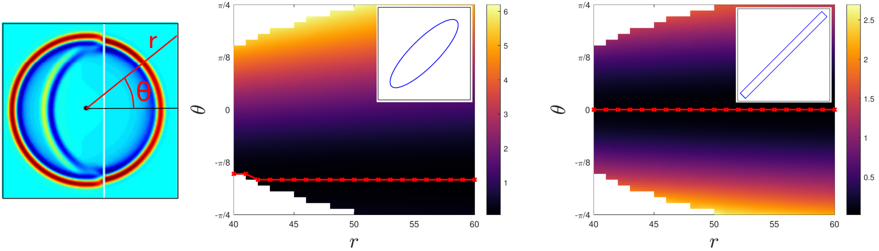

- "Attenuated direction" linked to the effective transmission coefficient $\mathcal{T}$ computed for a plane wave with wavenumber k and incident angle θ_I:

$$\mathcal{T}(\theta_\mathrm{I}) = 1 + \mathrm{i}(k\ell)\mathcal{T}_1(\boldsymbol{m}_\mathrm{eff}, \theta_\mathrm{I}) + O((k\ell)^2)$$

"Attenuated direction" at θ_min when $\mathcal{T}_1(\boldsymbol{m}_\mathrm{eff}, \theta_\mathrm{I})$ *changes sign* at $\theta_\mathrm{I} = \theta_\mathrm{min}$.

- Main cost functional:

$$\mathcal{J}_\mathrm{main}(\boldsymbol{m}_\mathrm{eff}) = \left(\frac{\mathcal{T}_1(\boldsymbol{m}_\mathrm{eff}, \theta_\mathrm{min})}{\partial_\theta \mathcal{T}_1(\boldsymbol{m}_\mathrm{eff}, \theta_\mathrm{min})} \right)^2 \quad \text{with} \quad \partial_\theta \mathcal{T}_1 = \frac{\partial \mathcal{T}_1}{\partial \theta_\mathrm{I}}$$

Results for $\theta_{\min} = 0$, $V_C = 0.2$, perimeter penalisation

Initialisations:

ellipse at $45°$

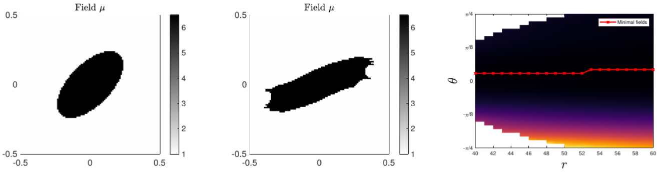

(d) (e) (f)

Random distribution

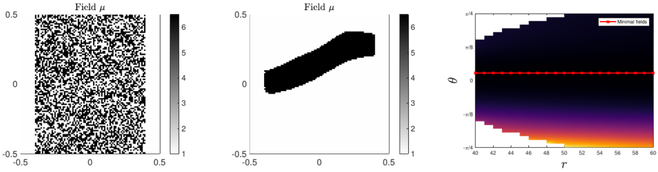

(g) (h) (i)

"Optimal" ellipse
(almost) analytical optimisation based on approximative $\boldsymbol{m}_{\text{eff}}$

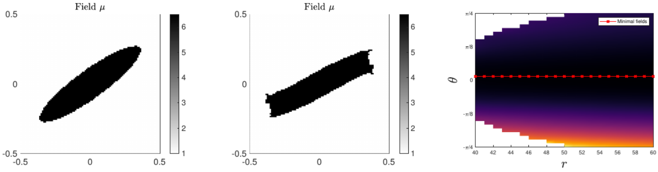

Performances for for $\theta_{\min} = 0$, $V_C = 0.2$

	N_{iter}	V end	$\mathcal{J}$ init.	$\mathcal{J}$ end	$\mathcal{J}_{\text{main}}$ init.	$\mathcal{J}_{\text{main}}$ end
ellipse	103	0.15	1.21	$2.24 \cdot 10^{-1}$	$9.72 \cdot 10^{-1}$	$1.4 \cdot 10^{-2}$
random	82	0.16	$5.23 \cdot 10^{3}$	$1.93 \cdot 10^{-1}$	$5.23 \cdot 10^{3}$	$7.2 \cdot 10^{-3}$
optimal ellipse	60	0.14	$1.02 \cdot 10^{-1}$	$6.76 \cdot 10^{-2}$	$3.61 \cdot 10^{-1}$	$2.1 \cdot 10^{-3}$

Results for $\theta_{\min} = \pi/4$, $V_C = 0.3$, perimeter penalisation

Initialisations:

ellipse at $45°$

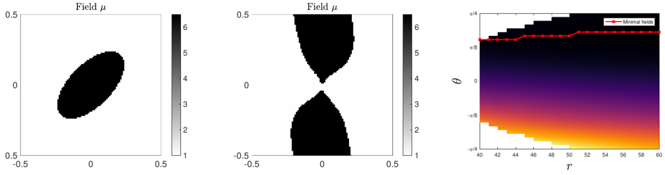

(a) (b) (c)

Random distribution

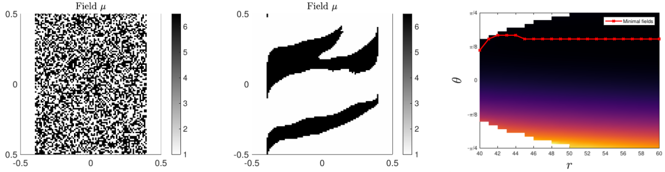

(d) (e) (f)

"Optimal" ellipse
(almost) analytical optimisation based on approximative $\boldsymbol{m}_{\text{eff}}$

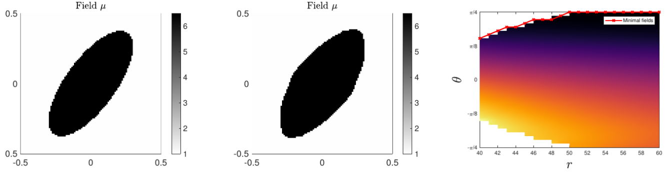

Performances for $\theta_{\min} = \pi/4$, $V_C = 0.3$:

	N_{iter}	V end	$\mathcal{J}$ init.	$\mathcal{J}$ end	$\mathcal{J}_{\text{main}}$ init.	$\mathcal{J}_{\text{main}}$ end
ellipse	49	0.30	1.51	$2.84 \cdot 10^{-2}$	1.40	$9.72 \cdot 10^{-5}$
random	52	0.24	$2.03 \cdot 10^{-1}$	$1.35 \cdot 10^{-1}$	$2.11 \cdot 10^{-4}$	$7.99 \cdot 10^{-4}$
optimal ellipse	28	0.28	$6.27 \cdot 10^{-2}$	$2.96 \cdot 10^{-2}$	$3.30 \cdot 10^{-3}$	$8.76 \cdot 10^{-5}$

Conclusions

- A topological optimization procedure is proposed, combining
  - Effective model obtained via two-scale asymptotic homogenization
  - FFT-based algorithms to solve cell problems
  - Approximative effective coefficients (for ellipses, using topological derivatives)
    $\Rightarrow$ Help to find specific initialisations.
  - Level-set, TD-based, projection algorithm (with volume and perimeter constraints)
- The procedure is applied to achieve
  - Minimal reflexion under volume constraint.
  - Attenuation of scattered energy in chosen direction.

Perspectives

- Time-domain simulations of waves in the designed materials
- Extensions to other other physics and regimes:
  1. **Elasticity**
  2. **Resonant interfaces** with high-contrast inclusions [Pham et al., 2017, Touboul et al., 2020] [Nicolas Lebbe, hier]
- Improve the optimization algorithm
  - Couple shape and topological derivative [Allaire et al., 2005, Amstutz et al., 2018]
  - Use optimized FFT solvers.

Merci pour votre attention !

Et à toutes les personnes qui œuvrent et ont œuvré pour le GDR MecaWave !

- *FFT-based computation of homogenized interface parameters*
  Rémi Cornaggia, Marie Touboul & Cédric Bellis
  Comptes Rendus Mécanique, 2022

- Marie Touboul's Ph.D. :
  Acoustic and elastic wave propagation in microstructured media with interfaces: homogenization, simulation and optimization
  https://tel.archives-ouvertes.fr/tel-03411353

- *Topological sensitivity-based analysis and optimization of microstructured interfaces*
  Marie Touboul, Rémi Cornaggia & Cédric Bellis
  Hopefully on HAL before summer ...

References

Allaire, G., de Gournay, F., Jouve, F., and Toader, A.-M. (2005).
Structural optimization using topological and shape sensitivity via a level set method.
Control and Cybernetics, 34(1):59–80.

Ammari, H. and Kang, H. (2007).
Polarization and moment tensors: with applications to inverse problems and effective medium theory, volume 162.
Springer.

Amstutz, S. (2011).
Analysis of a level set method for topology optimization.
Optimization Methods and Software, 26(4-5):555–573.

Amstutz, S. (2013).
Regularized perimeter for topology optimization.
SIAM Journal on Control and Optimization, 51(3):2176–2199.

Amstutz, S. and Andrä, H. (2006).
A new algorithm for topology optimization using a level-set method.
Journal of Computational Physics, 216(2):573 – 588.

Amstutz, S., Dapogny, C., and Ferrer, À. (2018).
A consistent relaxation of optimal design problems for coupling shape and topological derivatives.
Numerische Mathematik, 140(1):35–94.

Bonnet, M. (2009).
Higher-order topological sensitivity for 2-d potential problems. application to fast identification of inclusions.
International Journal of Solids and Structures, 46(11?12):2275 – 2292.

Bonnet, M., Cornaggia, R., and Guzina, B. (2018).
Microstructural topological sensitivities of the second-order macroscopic model for waves in periodic media.
SIAM Journal on Applied Mathematics, 78(4):2057–2082.

Cedio-Fengya, D. J., Moskow, S., and Vogelius, M. S. (1998).
Identification of conductivity imperfections of small diameter by boundary measurements. continuous dependence and computational reconstruction.
Inverse Problems, 14(3):553.

Eshelby, J. (1957).
The determination of the elastic field of an ellipsoidal inclusion, and related problems.
Proceedings of the Royal Society, 241:376–396.

Garreau, S., Guillaume, P., and Masmoudi, M. (2001).
The topological asymptotic for pde systems: The elasticity case.
SIAM Journal on Control and Optimization, 39(6):1756–1778.

Lombard, B., Maurel, A., and Marigo, J. (2017).
Numerical modeling of the acoustic wave propagation across a homogenized rigid microstructure in the time domain.
Journal of Computational Physics, 335:558 – 577.

Marigo, J.-J., Maurel, A., Pham, K., and Sbitti, A. (2017).
Effective dynamic properties of a row of elastic inclusions: The case of scalar shear waves.
Journal of Elasticity, 128(2):265–289.

Moulinec, H. and Suquet, P. (1995).
A FFT-based numerical method for computing the mechanical properties of composites from images of their microstructures.

In *IUTAM Symposium on Microstructure-Property Interactions in Composite Materials*, pages 235–246. Springer Netherlands.

Noguchi, Y. and Yamada, T. (2021).
Topology optimization of acoustic metasurfaces by using a two-scale homogenization method.
Applied Mathematical Modelling, 98:465–497.

Parnell, W. J. (2016).
The Eshelby, Hill, moment and concentration tensors for ellipsoidal inhomogeneities in the Newtonian potential problem and linear elastostatics.
Journal of Elasticity, pages 1–64.

Pham, K., Maurel, A., and Marigo, J.-J. (2017).
Two scale homogenization of a row of locally resonant inclusions - the case of anti-plane shear waves.
Journal of the Mechanics and Physics of Solids, 106:80 – 94.

Sokolowski, J. and Zochowski, A. (1999).
On the topological derivative in shape optimization.
SIAM Journal on Control and Optimization, 37(4):1251–1272.

Touboul, M., Pham, K., Maurel, A., Marigo, J.-J., Lombard, B., and Bellis, C. (2020).
Effective resonant model and simulations in the time-domain of wave scattering from a periodic row of highly-contrasted inclusions.
Journal of Elasticity, 142(1):53–82.